

## Inter-Peptide Hydrogen Bonding in Monolayers of Oligoglycine Amphiphiles

Xiao Cha, Katsuhiko Ariga, and Toyoki Kunitake<sup>\*,#</sup>

Supermolecules Project, JRDC, 2432 Aikawa, Kurume Research Center, Kurume, Fukuoka 839

(Received July 26, 1995)

*N*-Octadecanoyl oligoglycine (monomer to pentamer) ethyl esters were synthesized. The structures of their monolayers and LB films transferred from pure water were investigated by  $\pi$ -A isotherms and FT-IR reflection absorption spectroscopy (FT-IR, RAS). All the glycine residues were involved in intermolecular hydrogen bonding as indicated by shifts of the NH stretching band and other IR features. The strength of the hydrogen bonds was increased with increasing numbers of the glycine residues in a molecule. The FT-IR characteristics of these monolayers are close to those of polyglycine II, despite the fact that these oligopeptides are not long enough for conformational fixation in bulk water.

Hydrogen bonds play a most important role in defining precise three-dimensional structures of proteins and their supramolecular complexes. The nature and strength of the hydrogen bond in amino acids and peptides have been widely studied by various spectroscopic methods as bases for understanding protein-folding mechanisms, host-guest recognition, and enzymatic catalysis. Most of these investigations were done in isotropic environments, e.g., in homogeneous nonpolar media or in aqueous solution; however, many biological interactions occur at the macromolecular interface, especially at the surface of biomembranes. Organized molecular monolayers and bilayers are especially useful as mimics of these interactions occurring at the interface because they can provide uniquely oriented surface environments. Monolayers composed of peptides or polypeptides and peptide/lipid mixtures have been investigated extensively.<sup>1–7)</sup> Most of these papers were concerned with orientation, bioactivity, and intramolecular hydrogen bonding of the peptides and proteins involved. The problem of intermolecular hydrogen bonding among peptides and proteins in monolayers was taken up by Higashi et al.<sup>8)</sup> and by Röthlisberger et al.<sup>9)</sup> recently. The former group showed the presence of a  $\beta$ -like structure in compressed monolayers of poly(L-glutamic acid) derivatives; and the latter used molecular dynamics to study intermolecular hydrogen bonding of peptide moieties in self-assembling monolayers.

To conduct a systematic examination of inter- and intramolecular hydrogen bonding occurring in peptide monolayers, we synthesized a series of oligoglycine amphiphiles and investigated their monolayer properties and conformations at the air/water interface. The strength of intermolecular hydrogen bonds is enhanced with increasing numbers of the glycine residue. These results give us useful information

on how to design organized hydrogen bonding systems at the interface.

### Experimental

**Materials.** Glycine ethyl ester hydrochloride, glycyglycine, and triglycine were purchased from the Peptide Institute, Inc. Tetraglycine and pentaglycine were purchased from Sigma Chemical Co. They were used without further purification. The oligoglycine amphiphiles, C<sub>18</sub>Gly<sub>*n*</sub>OEt, were synthesized by esterification of oligoglycines followed by reaction with octadecanoyl chloride.

**Glycyglycine Ethyl Ester *p*-Toluenesulfonate (PTS Gly<sub>2</sub>OEt).** Glycyglycine (3.00 g, 22.7 mmol) and *p*-toluenesulfonic acid monohydrate (8.64 g, 45.4 mmol) were dissolved in 300 cm<sup>3</sup> of EtOH and refluxed for 4 h. After EtOH was evaporated, 100 cm<sup>3</sup> of acetone was added to the oily residue and evaporated again. The resulting white solid was dispersed in 150 cm<sup>3</sup> of hot acetone, and the insoluble product, 3.58 g (10.8 mmol), was collected by filtration after cooling. Yield 47.5%; mp 125.0–126.0 °C; <sup>1</sup>H NMR (300 MHz, DMSO-*d*<sub>6</sub>)  $\delta$  = 1.20 (t, *J* = 7.2 Hz, 3H, COOCH<sub>2</sub>CH<sub>3</sub>), 2.29 (s, 3H, Ar-CH<sub>3</sub>), 3.62 (s, 2H, glycine CH<sub>2</sub>), 3.95 (t, *J* = 2.9 Hz, 2H, glycine CH<sub>2</sub>), 4.11 (q, *J* = 7.1 Hz, 2H, COOCH<sub>2</sub>CH<sub>3</sub>), 7.11 (d, *J* = 7.5 Hz, 2H, Ar H), 7.47 (d, *J* = 8.1 Hz, 2H, Ar H), 8.04 (br, 3H, NH<sub>3</sub><sup>+</sup>), 8.76 (br, 1H, CONH). Found: C, 46.82; H, 6.00; N, 8.41%. Calcd for C<sub>13</sub>H<sub>20</sub>N<sub>2</sub>O<sub>6</sub>S: C, 46.98; H, 6.07; N, 8.43%.

PTS Gly<sub>3</sub>OEt, PTS Gly<sub>4</sub>OEt, and PTS Gly<sub>5</sub>OEt were obtained by similar procedures.

**Glycyglycyglycine Ethyl Ester *p*-Toluenesulfonate (PTS Gly<sub>3</sub>OEt).** Yield 72.2%; mp 142.0–142.5 °C; <sup>1</sup>H NMR (300 MHz, DMSO-*d*<sub>6</sub>)  $\delta$  = 1.18 (t, *J* = 7.1 Hz, 3H, COOCH<sub>2</sub>CH<sub>3</sub>), 2.28 (s, 3H, Ar-CH<sub>3</sub>), 3.59 (s, 2H, glycine CH<sub>2</sub>), 3.84 (m, 4H, 2 glycine CH<sub>2</sub>), 4.08 (q, *J* = 7.1 Hz, 2H, COOCH<sub>2</sub>CH<sub>3</sub>), 7.09 (d, *J* = 7.9 Hz, Ar H), 7.46 (d, *J* = 8.1 Hz, 2H, Ar H), 7.98 (br, 3H, NH<sub>3</sub><sup>+</sup>), 8.42 (br, 1H, CONH), 8.63 (br, 1H, CONH). Found: C, 46.06; H, 5.96; N, 10.79%. Calcd for C<sub>15</sub>H<sub>23</sub>N<sub>3</sub>O<sub>7</sub>S: C, 46.26; H, 5.95; N, 10.79%.

**Glycyglycyglycyglycine Ethyl Ester *p*-Toluenesulfonate (PTS Gly<sub>4</sub>OEt).** Yield 86.0%; mp 179.0–179.5 °C; <sup>1</sup>H NMR (300 MHz, DMSO-*d*<sub>6</sub>)  $\delta$  = 1.19 (t, *J* = 7.1 Hz, 3H, COOCH<sub>2</sub>CH<sub>3</sub>), 2.29 (s, 3H, Ar-CH<sub>3</sub>), 3.57 (m, 2H, glycine CH<sub>2</sub>), 3.74 (m, 2H,

<sup>#</sup>Permanent address: Faculty of Engineering, Kyushu University, Fukuoka 812.

glycine CH<sub>2</sub>), 3.84 (m, 4H, 2 glycine CH<sub>2</sub>), 4.09 (q,  $J = 7.2$  Hz, 2H, COOCH<sub>2</sub>CH<sub>3</sub>), 7.11 (d,  $J = 7.8$  Hz, 2H, Ar H), 7.47 (d,  $J = 8.1$  Hz, 2H, Ar H), 7.72 (br, 1H, CONH), 8.30 (br, 4H, NH<sub>3</sub><sup>+</sup>, CONH), 8.57 (br, 1H, CONH). Found: C, 45.63; H, 5.83; N, 12.45%. Calcd for C<sub>17</sub>H<sub>26</sub>N<sub>4</sub>O<sub>8</sub>S: C, 45.73; H, 5.87; N, 12.55%.

**Glycylglycylglycylglycylglycine Ethyl Ester *p*-Toluenesulfonate (PTS Gly<sub>5</sub>OEt).** Yield 78.2%; mp 191.0–192.0 °C;

<sup>1</sup>H NMR (300 MHz, DMSO-*d*<sub>6</sub>)  $\delta = 1.19$  (t,  $J = 7.1$  Hz, 3H, COOCH<sub>2</sub>CH<sub>3</sub>), 2.28 (s, 3H, Ar-CH<sub>3</sub>), 3.61 (s, 2H, glycine CH<sub>2</sub>), 3.76 (m, 4H, 2 glycine CH<sub>2</sub>), 3.84 (m, 4H, 2 glycine CH<sub>2</sub>), 4.09 (q,  $J = 6.9$  Hz, 2H, COOCH<sub>2</sub>CH<sub>3</sub>), 7.11 (d,  $J = 7.8$  Hz, 2H, Ar H), 7.47 (d,  $J = 7.8$  Hz, 2H, Ar H), 8.00 (br, 3H, NH<sub>3</sub><sup>+</sup>), 8.19 (br, 1H, CONH), 8.29 (br, 2H, 2 CONH), 8.61 (br, 1H, CONH). Found: C, 44.56; H, 5.79; N, 13.59%. Calcd for C<sub>19</sub>H<sub>29</sub>N<sub>5</sub>O<sub>9</sub>S·1/2H<sub>2</sub>O: C, 44.53; H, 5.90; N, 13.66%.

***N*-Octadecanoylglycylglycine Ethyl Ester (C<sub>18</sub>Gly<sub>2</sub>OEt).** PTS Gly<sub>2</sub>OEt (0.20 g, 0.60 mmol) and triethylamine (0.50 cm<sup>3</sup>, 3.59 mmol) were dissolved in 50 cm<sup>3</sup> of CH<sub>2</sub>Cl<sub>2</sub>, and 0.25 cm<sup>3</sup> (0.74 mmol) of stearoyl chloride was added. The reaction mixture was stirred for 21 h in a 1000 cm<sup>3</sup> Erlenmeyer flask with a CaCl<sub>2</sub> tube. The solution turned turbid and viscous during the reaction. After the solvent was evaporated, the resulting white solid was washed with dilute hydrochloric acid and ethyl ether. Recrystallization from 10 cm<sup>3</sup> of CH<sub>2</sub>Cl<sub>2</sub> gave 0.15 g (0.41 mmol) of the product as colorless solid. Yield 59%; mp 129.5–130.0 °C; <sup>1</sup>H NMR (300 MHz, DMSO-*d*<sub>6</sub>)  $\delta = 0.86$  (t,  $J = 7.1$  Hz, 3H, COCH<sub>2</sub>CH<sub>2</sub>(CH<sub>2</sub>)<sub>14</sub>CH<sub>3</sub>), 1.18 (t,  $J = 7.1$  Hz, 3H, COOCH<sub>2</sub>CH<sub>3</sub>), 1.24 (m, 28H, COCH<sub>2</sub>CH<sub>2</sub>(CH<sub>2</sub>)<sub>14</sub>CH<sub>3</sub>), 1.47 (br, 2H, COCH<sub>2</sub>CH<sub>2</sub>(CH<sub>2</sub>)<sub>14</sub>CH<sub>3</sub>), 2.11 (t,  $J = 7.5$  Hz, 2H, COCH<sub>2</sub>CH<sub>2</sub>(CH<sub>2</sub>)<sub>14</sub>CH<sub>3</sub>), 3.70 (d,  $J = 4.7$  Hz, 2H, glycine CH<sub>2</sub>), 3.82 (d,  $J = 5.8$  Hz, 2H, glycine CH<sub>2</sub>), 4.08 (q,  $J = 7.0$  Hz, 2H, COOCH<sub>2</sub>CH<sub>3</sub>), 8.05 (br, 1H, CONH), 8.21 (br, 1H, CONH). Found: C, 66.91; H, 10.69; N, 6.63%. Calcd for C<sub>24</sub>H<sub>46</sub>N<sub>2</sub>O<sub>4</sub>·1/4H<sub>2</sub>O: C, 66.86; H, 10.87; N, 6.50%.

C<sub>18</sub>GlyOEt, C<sub>18</sub>Gly<sub>3</sub>OEt, C<sub>18</sub>Gly<sub>4</sub>OEt, and C<sub>18</sub>Gly<sub>5</sub>OEt were obtained by similar procedures. In the synthesis of C<sub>18</sub>GlyOEt, commercially available glycine ethyl ester hydrochloride was used instead of PTS GlyOEt. Dry DMF was used as the solvent in the case of C<sub>18</sub>GlyOEt, C<sub>18</sub>Gly<sub>4</sub>OEt, and C<sub>18</sub>Gly<sub>5</sub>OEt.

***N*-Octadecanoylglycine Ethyl Ester (C<sub>18</sub>GlyOEt).** Yield 92.0%; mp 83.0–83.5 °C; <sup>1</sup>H NMR (300 MHz, CDCl<sub>3</sub>)  $\delta = 0.88$  (t,  $J = 6.7$  Hz, 3H, COCH<sub>2</sub>CH<sub>2</sub>(CH<sub>2</sub>)<sub>14</sub>CH<sub>3</sub>), 1.25 (m, 28H, COCH<sub>2</sub>CH<sub>2</sub>(CH<sub>2</sub>)<sub>14</sub>CH<sub>3</sub>), 1.29 (t,  $J = 7.1$  Hz, 3H, COOCH<sub>2</sub>CH<sub>3</sub>), 1.62 (t,  $J = 7.5$  Hz, 2H, COCH<sub>2</sub>CH<sub>2</sub>(CH<sub>2</sub>)<sub>14</sub>CH<sub>3</sub>), 2.36 (t,  $J = 7.6$  Hz, COCH<sub>2</sub>CH<sub>2</sub>(CH<sub>2</sub>)<sub>14</sub>CH<sub>3</sub>), 4.04 (d,  $J = 5.0$  Hz, 2H, glycine CH<sub>2</sub>), 4.22 (q,  $J = 7.1$  Hz, 2H, COOCH<sub>2</sub>CH<sub>3</sub>), 5.92 (br, 1H, CONH). Found: C, 70.94; H, 11.64; N, 3.75%. Calcd for C<sub>22</sub>H<sub>43</sub>NO<sub>3</sub>·1/4H<sub>2</sub>O: C, 70.64; H, 11.72; N, 3.74%.

***N*-Octadecanoylglycylglycylglycine Ethyl Ester (C<sub>18</sub>Gly<sub>3</sub>OEt).** Yield 35.7%; mp 200.8–201.3 °C; <sup>1</sup>H NMR (300 MHz, DMSO-*d*<sub>6</sub>)  $\delta = 0.85$  (t,  $J = 5.9$  Hz, 3H, COCH<sub>2</sub>CH<sub>2</sub>(CH<sub>2</sub>)<sub>14</sub>CH<sub>3</sub>), 1.19 (t,  $J = 7.1$  Hz, 3H, COOCH<sub>2</sub>CH<sub>3</sub>), 1.23 (m, 28H, COCH<sub>2</sub>CH<sub>2</sub>(CH<sub>2</sub>)<sub>14</sub>CH<sub>3</sub>), 1.47 (br, 2H, COCH<sub>2</sub>CH<sub>2</sub>(CH<sub>2</sub>)<sub>14</sub>CH<sub>3</sub>), 2.11 (t,  $J = 7.7$  Hz, 2H, COCH<sub>2</sub>CH<sub>2</sub>(CH<sub>2</sub>)<sub>14</sub>CH<sub>3</sub>), 3.72 (m, 4H, 2 glycine CH<sub>2</sub>), 3.82 (d,  $J = 5.4$  Hz, 2H, glycine CH<sub>2</sub>), 4.09 (q,  $J = 7.1$  Hz, 2H, COOCH<sub>2</sub>CH<sub>3</sub>), 8.05 (br, 1H, CONH), 8.12 (br, 1H, CONH), 8.24 (br, 1H, CONH). Found: C, 63.36; H, 9.96; N, 8.65%. Calcd for C<sub>26</sub>H<sub>49</sub>N<sub>3</sub>O<sub>5</sub>·1/2H<sub>2</sub>O: C, 63.38; H, 10.23; N, 8.53%.

***N*-Octadecanoylglycylglycylglycylglycine Ethyl Ester (C<sub>18</sub>Gly<sub>4</sub>OEt).** Yield 58.8%; mp 266 °C (decomp); <sup>1</sup>H NMR (300 MHz, DMSO-*d*<sub>6</sub>)  $\delta = 0.87$  (t,  $J = 6.5$  Hz, 3H, COCH<sub>2</sub>CH<sub>2</sub>(CH<sub>2</sub>)<sub>14</sub>CH<sub>3</sub>), 1.21 (t,  $J = 7.1$  Hz, 3H,

COOCH<sub>2</sub>CH<sub>3</sub>), 1.27 (m, 28H, COCH<sub>2</sub>CH<sub>2</sub>(CH<sub>2</sub>)<sub>14</sub>CH<sub>3</sub>), 1.53 (br, 2H, COCH<sub>2</sub>CH<sub>2</sub>(CH<sub>2</sub>)<sub>14</sub>CH<sub>3</sub>), 2.15 (t,  $J = 7.3$  Hz, 2H, COCH<sub>2</sub>CH<sub>2</sub>(CH<sub>2</sub>)<sub>14</sub>CH<sub>3</sub>), 3.76 (m, 6H, 3 glycine CH<sub>2</sub>), 3.83 (m, 2H, glycine CH<sub>2</sub>), 4.12 (q,  $J = 7.0$  Hz, 2H, COOCH<sub>2</sub>CH<sub>3</sub>), 7.77 (br, 4H, 4 CONH). Found: C, 61.76; H, 9.61; N, 10.17%. Calcd for C<sub>28</sub>H<sub>52</sub>N<sub>4</sub>O<sub>6</sub>·1/4H<sub>2</sub>O: C, 61.68; H, 9.71; N, 10.28%.

***N*-Octadecanoylglycylglycylglycylglycylglycine Ethyl Ester (C<sub>18</sub>Gly<sub>5</sub>OEt).** Yield 47.0%; mp 250 °C (decomp); <sup>1</sup>H NMR (300 MHz, DMSO-*d*<sub>6</sub>)  $\delta = 0.84$  (t,  $J = 6.6$  Hz, 3H, COCH<sub>2</sub>CH<sub>2</sub>(CH<sub>2</sub>)<sub>14</sub>CH<sub>3</sub>), 1.17 (t,  $J = 7.1$  Hz, 3H, COOCH<sub>2</sub>CH<sub>3</sub>), 1.22 (m, 28H, COCH<sub>2</sub>CH<sub>2</sub>(CH<sub>2</sub>)<sub>14</sub>CH<sub>3</sub>), 1.46 (br, 2H, COCH<sub>2</sub>CH<sub>2</sub>(CH<sub>2</sub>)<sub>14</sub>CH<sub>3</sub>), 2.10 (t,  $J = 7.4$  Hz, 2H, COCH<sub>2</sub>CH<sub>2</sub>(CH<sub>2</sub>)<sub>14</sub>CH<sub>3</sub>), 3.69 (m, 2H, glycine CH<sub>2</sub>), 3.72 (m, 6H, 3 glycine CH<sub>2</sub>), 3.81 (m, 2H, glycine CH<sub>2</sub>), 4.07 (q,  $J = 7.1$  Hz, 2H, COOCH<sub>2</sub>CH<sub>3</sub>), 8.08 (m, 4H, 4 CONH), 8.23 (br, 1H, CONH). Found: C, 58.98; H, 9.04; N, 11.36%. Calcd for C<sub>30</sub>H<sub>55</sub>N<sub>5</sub>O<sub>7</sub>·2/3H<sub>2</sub>O: C, 59.09; H, 9.31; N, 11.48%.

**Pressure-Area Isotherms.** A computer-controlled film balance system, FSD-110 (trough size, 100×200 mm<sup>2</sup>, USI system, Japan), was used.  $\pi$ -*A* Isotherms were taken at a compression rate of 4 mm min<sup>−1</sup> and a subphase temperature of 20.0±0.3 °C. The subphase water was deionized and doubly distilled. The spreading solutions of oligoglycine amphiphiles were 0.16 mg cm<sup>−3</sup> in CF<sub>3</sub>COOH–chloroform (2:98 by volume).

**LB Films.** Monolayers were transferred onto Au-deposited glass slides or onto CaF<sub>2</sub> plates in the vertical mode at a surface pressure of 20 mN m<sup>−1</sup> and at up-stroke and down-stroke motions of 8 and 100 mm min<sup>−1</sup>, respectively, from pure water as the subphase. The transfer ratio was 1.0±0.1 in the up-stroke mode but there was no transfer in the down-stroke mode.

**FT-IR Measurements.** Infrared spectra were obtained on an FT-IR spectrometer (Nicolet 710) with a MCT detector (for RAS, reflection absorption spectroscopy) or with a DTGS detector (for the transmission method). All data for C<sub>18</sub>GlyOEt, C<sub>18</sub>Gly<sub>2</sub>OEt, C<sub>18</sub>Gly<sub>3</sub>OEt, and C<sub>18</sub>Gly<sub>5</sub>OEt were collected by the RAS method. The data for C<sub>18</sub>Gly<sub>4</sub>OEt were collected by both of the RAS and transmission methods. The transmission absorption spectrum was similar to its RAS spectrum except for relative intensities between some peaks including amide I and amide II, and these peak intensities were much weaker than those from RAS. Peaks ascribed to CH<sub>2</sub> twisting and wagging vibrations of the glycine residues were more clearly seen in reflection spectra, thus we mainly used the RAS method to evaluate the LB film structure.

## Results and Discussion

**Monolayer Behavior.** Polyglycine is not soluble in pure water because of their strong intermolecular hydrogen bonding, although commercially available oligoglycines such as diglycine to pentaglycine can be easily dissolved in water. The number of the intermolecular hydrogen bonds should increase with the increase in the glycine residues in amphiphiles C<sub>18</sub>Gly<sub>*n*</sub>OEt, (*n* = 1–5). These hydrogen bonds together with the hydrophobic packing force among alkyl chains make these amphiphiles high melting (see Experimental Section) and hardly soluble in water and in organic solvents including DMF, DMSO, THF, chloroform, and benzene. It was possible to spread these amphiphiles onto a water surface only by using a mixed solvent of CF<sub>3</sub>COOH (TFA) and CHCl<sub>3</sub>, (2:98 by volume, the amphiphiles were dissolved first in TFA and then diluted by CHCl<sub>3</sub>).

$\pi$ - $A$  Isotherms of  $C_{18}GlyOEt$ ,  $C_{18}Gly_3OEt$ , and  $C_{18}Gly_5OEt$  monolayers are shown in Fig. 1.  $\pi$ - $A$  patterns of amphiphiles  $C_{18}Gly_2OEt$  and  $C_{18}Gly_4OEt$  are essentially the same as that of  $C_{18}GlyOEt$  monolayer. None of these isotherms show expanded phases. The limiting areas are 29.7, 29.8, 29.1, 29.0, and 30.0  $\text{\AA}^2$ , respectively, for  $C_{18}GlyOEt$ ,  $C_{18}Gly_2OEt$ ,  $C_{18}Gly_3OEt$ ,  $C_{18}Gly_4OEt$ , and  $C_{18}Gly_5OEt$  monolayers. These limiting areas are larger than that of stearic acid monolayer (20  $\text{\AA}^2$ ), and it is suggested that the monolayer components are tilted more than the case of stearic acid on water. These close limiting areas imply that a common packing structure exists for these monolayers. The monolayers of  $C_{18}GlyOEt$ ,  $C_{18}Gly_2OEt$ , and  $C_{18}Gly_4OEt$  show collapse pressures at about 30  $\text{mN m}^{-1}$ , and  $C_{18}Gly_3OEt$  and  $C_{18}Gly_5OEt$  monolayers show collapse pressures at around 40  $\text{mN m}^{-1}$ . Destruction of the monolayers is noticed visually at surface pressures lower than the collapse pressure. LB films of  $C_{18}Gly_nOEt$  ( $n=1-5$ ) monolayers transferred from pure water are deposited as Z types, i.e., the monolayers are deposited only in the upstroke motion.

**IR Spectroscopic Data of LB Films.** FT-IR spectra of LB films of  $C_{18}Gly_nOEt$  ( $n=1-5$ ) monolayers transferred from pure water are shown for the region of 1800–1000  $\text{cm}^{-1}$  in Fig. 2 and 3400–3200  $\text{cm}^{-1}$  in Fig. 3. The NH stretching vibrations ( $\nu_{NH}$ ) are located at 3325–3294  $\text{cm}^{-1}$ . The antisymmetric and symmetric  $CH_2$  stretching bands are located at 2918 and 2850  $\text{cm}^{-1}$ , respectively. Their intensities in RAS are decreased with increasing numbers of the glycine residues in a molecule, which implies the lipid chains become less tilted with increasing numbers of glycine residues.<sup>10</sup> The ester carbonyl stretching is found commonly at 1740  $\text{cm}^{-1}$ , with an additional shoulder at 1750  $\text{cm}^{-1}$  in the case of  $C_{18}Gly_2OEt$  monolayers. The amide I band is at 1647  $\text{cm}^{-1}$  for  $C_{18}GlyOEt$  monolayer, at 1655 and 1637  $\text{cm}^{-1}$  for  $C_{18}Gly_2OEt$  monolayer, and at 1653  $\text{cm}^{-1}$  with a shoulder at 1637  $\text{cm}^{-1}$  for  $C_{18}Gly_nOEt$  ( $n=3-5$ ) monolayers. The amide II band is very intense compared with the amide I band, and is at 1552–1564  $\text{cm}^{-1}$ , shifting to higher frequencies with increasing numbers of glycine residues per molecule. However, the amide I band has a much stronger in-

tensity in the transmission spectrum (figure not shown) than that in the RAS. Since the electric field of IR radiation in the transmission measurement is parallel to the film surface and that in the RAS is perpendicular,<sup>10</sup> these results suggest that the oligoglycine moiety orient almost perpendicular to the film surface with their tilted lipid chains. The  $CH_2$  bending vibration is found commonly at 1420  $\text{cm}^{-1}$  (weak), and the corresponding wagging and twisting vibrations are at 1377  $\text{cm}^{-1}$  (wag), ca. 1289  $\text{cm}^{-1}$  and ca. 1250  $\text{cm}^{-1}$  (twist), respectively. The C–O stretching vibration of the ester group

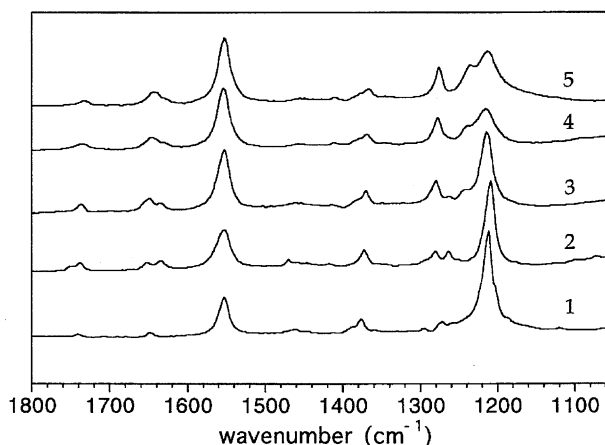


Fig. 2. FT-IR-RAS spectra of LB films of  $C_{18}Gly_nOEt$  monolayers transferred from pure water in the region of 1000–1800  $\text{cm}^{-1}$ , 12 layers. (1)  $C_{18}GlyOEt$ , (2)  $C_{18}Gly_2OEt$ , (3)  $C_{18}Gly_3OEt$ , (4)  $C_{18}Gly_4OEt$ , (5)  $C_{18}Gly_5OEt$ .

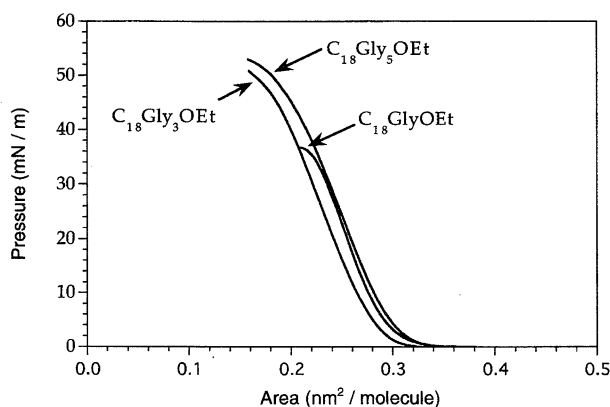


Fig. 1.  $\pi$ - $A$  isotherms of  $C_{18}Gly_nOEt$  monolayers on pure water,  $20 \pm 0.2^\circ\text{C}$ .

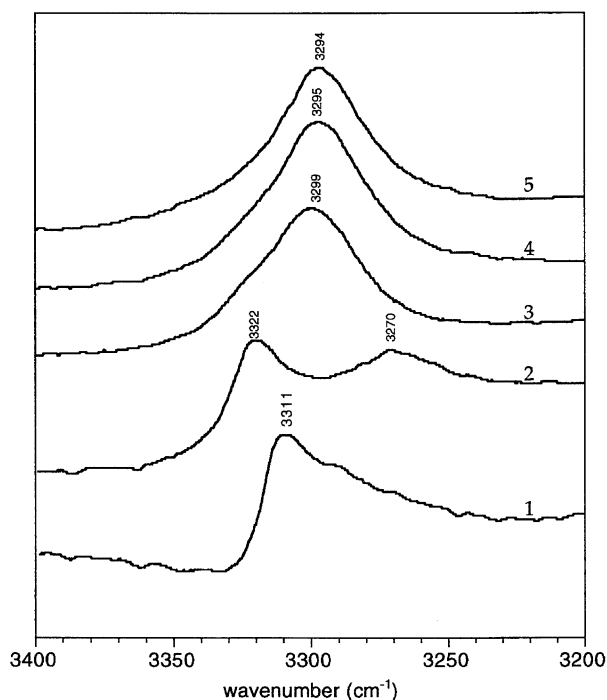


Fig. 3. FT-IR-RAS spectra of LB films of  $C_{18}Gly_nOEt$  monolayers transferred from pure water in the region of 3200–3400  $\text{cm}^{-1}$ , 12 layers. (1)  $C_{18}GlyOEt$ , (2)  $C_{18}Gly_2OEt$ , (3)  $C_{18}Gly_3OEt$ , (4)  $C_{18}Gly_4OEt$ , (5)  $C_{18}Gly_5OEt$ .

is very intense at  $1205\text{ cm}^{-1}$ . It is interesting that the IR spectrum of  $\text{C}_{18}\text{Gly}_2\text{OEt}$  is somewhat different from those of the other oligoglycine derivatives, but is similar to those reported for other diglycine derivatives and for triglycine. For instance, triglycine has two amide groups, and its IR spectrum shows two  $\nu_{\text{NH}}$  peaks at  $3310\text{--}3280\text{ cm}^{-1}$  and two  $\text{CH}_2\text{tw}$  at  $1260\text{--}1290\text{ cm}^{-1}$ .<sup>11,12)</sup>

#### Peptide Conformation in Oligoglycine Monolayers.

The  $\nu_{\text{NH}}$  frequencies of the LB films of these amphiphiles are lower than  $3330\text{ cm}^{-1}$ , and indicate that all the glycine residues in the amphiphiles are engaged in hydrogen bonding.<sup>13)</sup> Because the amphiphile molecules in compressed monolayers are oriented in one direction at the air/water interface, the glycine residues can form only parallel  $\beta$ -like or helix-like structures when the number of the glycine residue is two or greater. It is useful to compare IR frequencies of these LB films with those of polyglycine in order to study the nature of hydrogen bonding and the conformation of the polar oligoglycine moiety. Polyglycines  $((\text{Gly})_n)$  can usually assume two kinds of conformations in the solid-state:  $(\text{Gly})_n\text{I}$  ( $\beta$ -antiparallel form) and  $(\text{Gly})_n\text{II}$  ( $3_1$ -helical form), as confirmed by X-ray structure analysis.<sup>14–16)</sup> The glycine residues are involved in hydrogen bonding in both cases. The parallel polyglycine  $\beta$ -sheet has not been observed up to now, although this structure has been proposed by Bandekar and Krimm.<sup>17)</sup> According to their calculation, IR frequencies of the parallel polyglycine rippled sheet are almost identical to those of antiparallel  $(\text{Gly})_n\text{I}$ . Table 1 contains the observed and calculated IR frequencies of the antiparallel  $(\text{Gly})_n\text{I}$ , the observed and calculated frequencies of the parallel  $(\text{Gly})_n\text{II}$ , and the observed frequencies of  $\text{C}_{18}\text{Gly}_n\text{OEt}$ . By comparing these frequencies, we can see that most of IR frequencies for LB films of  $\text{C}_{18}\text{Gly}_n\text{OEt}$  ( $n=3\text{--}5$ ) are close or identical to those of  $(\text{Gly})_n\text{II}$  (parallel). Taking  $\text{C}_{18}\text{Gly}_4\text{OEt}$  as an example, its  $\nu_{\text{NH}}$  frequency is  $3295\text{ cm}^{-1}$  ( $3293\text{ cm}^{-1}$  in the transmission spectrum, data not shown). Since the  $\nu_{\text{NH}}$  peak of crystalline  $(\text{Gly})_n\text{II}$  is at  $3281\text{ cm}^{-1}$ , the inter-peptide hydrogen bonding in  $\text{C}_{18}\text{Gly}_4\text{OEt}$  appears weaker. The amide I band ( $1653\text{ cm}^{-1}$ ,  $1649\text{ cm}^{-1}$  in transmission spectra) with a shoulder at  $1637\text{ cm}^{-1}$  is close to the calculated ( $1649\text{ cm}^{-1}$ ) and observed ( $1640\text{ cm}^{-1}$ ) values for  $(\text{Gly})_n\text{II}$  rather than those for  $(\text{Gly})_n\text{I}$  (observed at  $1685$  and  $1636\text{ cm}^{-1}$ ). Amide II band is at  $1564\text{ cm}^{-1}$  for amphiphile  $\text{C}_{18}\text{Gly}_4\text{OEt}$  ( $1552\text{ cm}^{-1}$  in transmission spectra.), which is close to calculated ( $1551\text{ cm}^{-1}$ ) and observed ( $1550\text{ cm}^{-1}$ ) values of that for  $(\text{Gly})_n\text{II}$  ( $1517\text{ cm}^{-1}$  for  $(\text{Gly})_n\text{I}$ , observed). In the  $\text{CH}_2\text{b}$ ,  $\text{CH}_2\text{w}$  and  $\text{CH}_2\text{tw}$  region, LB films of  $\text{C}_{18}\text{Gly}_n\text{OEt}$  ( $n=3\text{--}5$ ) monolayers give almost the same peak positions as  $(\text{Gly})_n\text{II}$ . Among these peaks, the peaks at  $1420$  and  $1378\text{ cm}^{-1}$  are mainly attributed to  $\text{CH}_2$  of alkyl chains, and the peaks at  $1288$  and  $1250\text{ cm}^{-1}$  are attributed to  $\text{CH}_2$  of the glycine residues because their intensities increase with increasing numbers of the glycine residues. These monolayer peaks have counterparts at  $1420$ ,  $1377$ ,  $1283$ , and  $1249\text{ cm}^{-1}$  of  $(\text{Gly})_n\text{II}$ . In contrast,  $(\text{Gly})_n\text{I}$  gives corresponding peaks at  $1432\text{ cm}^{-1}$  ( $\text{CH}_2\text{b}$ ),  $1338\text{ cm}^{-1}$  ( $\text{CH}_2\text{w}$ ),  $1295$ , and  $1236\text{ cm}^{-1}$  ( $\text{CH}_2\text{tw}$ ), and these peaks are absent in the monolayer

Table 1. IR Characteristics of Polyglycines (I and II) and Monolayers of Oligoglycine Amphiphiles ( $\text{cm}^{-1}$ )<sup>a)</sup>

Assignments	(Gly) <sub>n</sub> I	(Gly) <sub>n</sub> II	LB films of C <sub>18</sub> (Gly) <sub>n</sub> OEt, obsd					
	Obsd	Obsd						
	antiparallel	parallel						
	β-sheet (Calcd)	3 <sub>1</sub> -helix (Calcd)	<i>n</i> :	1	2	3	4	5
NH	3284	3281	3311	3322	3299	3295	3294	
(str)	(3272)	(3279)		3270				
CH <sub>2</sub>	2931	2936	2918	2918	2918	2918	2918	
(asym str)	(2928)	(2935)						
CH <sub>2</sub>	2869	2850	2850	2850	2850	2850	2850	
(sym str)	(2861)	(2853)						
Amide I	1685 (1689)	—	—	—	—	—	—	—
	1636 (1643)	1640 (1649)	1647	1655	1653	1653	1653	
				1637	1637	1637	1637	
Amide II	1517 (1515)	1550 (1551)	1552	1555	1561	1564	1564	
CH <sub>2</sub>	1432 (1439)	1420 (—)	—	1422	1420	1420	1420	
(bend)								
CH <sub>2</sub>	1338 (1341)	1377 (1374)	1376	1377	1377	1378	1377	
(wag)								
CH <sub>2</sub>	1295 (1286)	1283 (1290)	1295	1268	1289	1288	1287	
(twist)				1285				
	1236 (1242)	1249 (1247)	1272	1256	1250	1250	1248	

a) Observed and calculated IR data of  $(\text{Gly})_n\text{I}$  and  $(\text{Gly})_n\text{II}$  are taken from Refs. 17, 22—27.

spectra.

We also compared IR characteristics of the monolayers with those of glycine homopeptides and glycine homopeptide ester hydrochlorides. The oligoglycines assume conformations identical to those of  $(\text{Gly})_n\text{I}$  and  $(\text{Gly})_n\text{II}$ , although the former conformations are often interconverted between  $\beta$ -sheet and  $3_1$ -helix depending on preparative conditions and the modification of the terminal group.<sup>18–20)</sup> In these cases, the  $\nu_{\text{NH}}$  and amide I frequencies of diglycine to hexaglycine are often composed of multiple peaks and their positions change irregularly. From triglycine to hexaglycine, there are two amide I peaks: a strong one is around  $1635\text{ cm}^{-1}$ , another medium one is around  $1665\text{ cm}^{-1}$ . Very broad amide II peaks are found for tetraglycine and pentaglycine around  $1540\text{ cm}^{-1}$ . All of these oligoglycines have the  $\text{CH}_2\text{w}$  peaks with very weak intensities at  $1350\text{--}1385\text{ cm}^{-1}$  (this peak is commonly assigned to the  $(\text{Gly})_n\text{II}$  structure), and the  $\text{CH}_2\text{b}$  peaks with medium intensity at  $1439\text{--}1453\text{ cm}^{-1}$  (this peak is commonly assigned to the  $(\text{Gly})_n\text{I}$  structure). These results suggest that the glycine homopeptides may have mixed structures made of  $\beta$ -sheet and  $3_1$ -helix. From these IR characteristics of the monolayers we can see that (1) all the amide NH groups in  $\text{C}_{18}\text{Gly}_n\text{OEt}$  are engaged in hydrogen bonding; (2) the hydrogen-bonded glycine residues should be in a parallel form; (3) the oligoglycine moieties are not in  $\beta$ -sheet conformation: Amide peaks are rather close to those in  $(\text{Gly})_n\text{II}$ . From these data, we conclude that  $\text{C}_{18}\text{Gly}_n\text{OEt}$  ( $n=3\text{--}5$ ) monolayers tend to form a parallel  $(\text{Gly})_n\text{II}$ -like

structure. This conformational restriction is derived from parallel orientation of the glycine residues at the air/water interface and the alkyl chain packing (consequently, oligoglycine packing) in compressed monolayers.

**Intermolecular Hydrogen Bonding.** Figure 3 shows the expanded  $\nu_{\text{NH}}$  region. It is apparent that the peak position is shifted to lower frequencies as the number of glycine residues increases. This indicates that the strength of hydrogen bonds among the glycine residues is increased with increasing numbers of the residues. This supposition is also supported by the fact that the amide II peak shifts to higher frequencies with increasing glycine residues. In addition to this general trend, there are IR characteristics specific to individual oligoglycine residues. The influence of the intermolecular hydrogen bonding appears very limited for  $\text{C}_{18}\text{GlyOEt}$  as the  $\nu_{\text{NH}}$  peak is located at  $3311\text{ cm}^{-1}$ .  $\text{C}_{18}\text{Gly}_2\text{OEt}$  gives two  $\nu_{\text{NH}}$  peaks at  $3322$  and  $3270\text{ cm}^{-1}$ . The former peak suggests weak hydrogen bonding and is probably attributed to the terminal glycine residue. The latter low frequency peak can be ascribed to the strongly hydrogen bonded, inner glycine residue. The  $\nu_{\text{NH}}$  peaks for longer glycine residues,  $\text{Gly}_3$  to  $\text{Gly}_5$ , are at almost identical positions ( $3299$  to  $3294\text{ cm}^{-1}$ ), although slight frequency increases with increasing glycine residues are noted. There lower frequency peaks are indicative of strong hydrogen bonding. The  $\nu_{\text{NH}}$  and amide II bands of  $\text{C}_{18}\text{Gly}_4\text{OEt}$  and  $\text{C}_{18}\text{Gly}_5\text{OEt}$  are located at identical positions. Apparently, the intermolecular hydrogen bonding at the interface becomes saturated at this glycine length, although the extent of the amide interaction is still weaker than those of polyglycines I and II ( $\nu_{\text{NH}}$  at  $3281$ – $3284\text{ cm}^{-1}$ ).

### Concluding Remarks

Figure 4 displays a conceivable model for the monolayer of oligoglycine amphiphiles by using  $\text{C}_{18}\text{Gly}_3\text{OEt}$  as a typical example. The packed alkyl chains on the water surface help their  $\text{Gly}_3$  moieties form hydrogen bonds with each other, and especially, the strengths of these hydrogen bonds can be increased with increasing numbers of the glycine residue in an amphiphile. The limiting area of a molecule is larger than either the standard cross section of the alkyl chain ( $20\text{ \AA}^2$ ) or the cross section ( $18.1\text{ \AA}^2$ ) of the glycyI chain in the  $(\text{Gly})_n\text{II}$  crystal. These area differences imply that the alkyl chains in the monolayer are packed in a tilted arrangement and that the intermolecular hydrogen bonding is longer and weaker at the interface than those in crystal.

The arrangement and conformation of peptide chains at the air–water interface provide an important research problem in relation to the behavior of peptide chains on the surface of biomembranes and other biological supramolecular systems. However, very few papers have been published on monolayers of well-characterized peptide amphiphiles. As a rare exception, Higashi et al.<sup>8)</sup> studied the structure of the poly(L-glutamic acid) moiety appended to double alkyl chains at the air/water interface, and found that a stable  $\beta$ -structure was formed in the condensed phase when the peptide moiety (degree of polymerization ca. 40) was aligned in monolayers. Conventional poly(L-glutamic acid) displays a conformational transition between  $\alpha$ -helix and random coil, depending on pH, solvent composition, and temperature.<sup>28)</sup> It is clear that spatial confinement and chain alignment at the interface induced the  $\beta$ -structure rather than the conventional  $\alpha$ -helix. Our study provides an additional example of a pep-

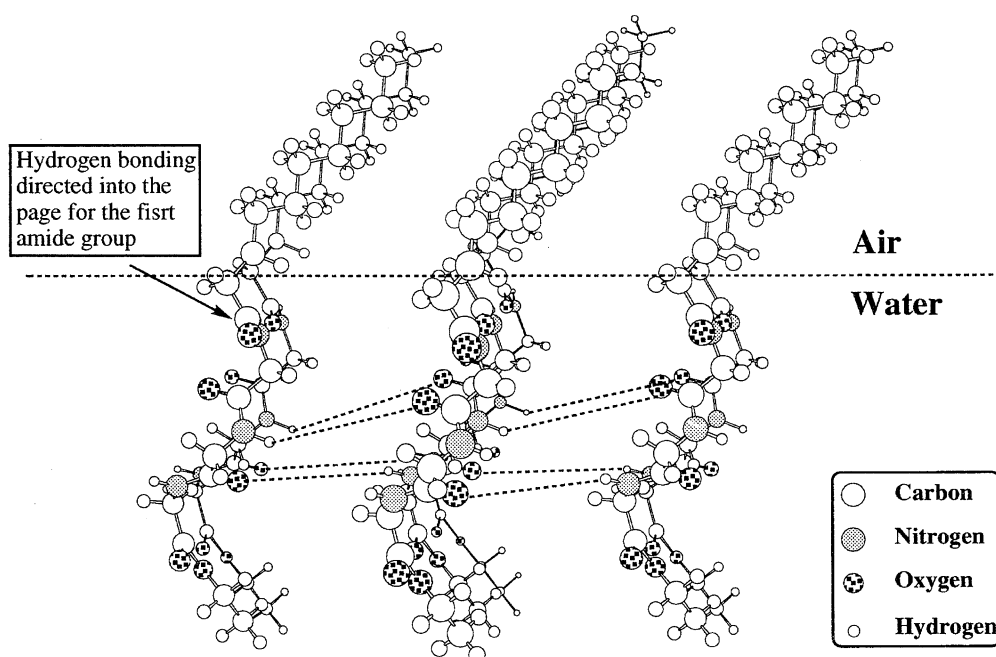


Fig. 4. A schematic representation of molecular packing and the pattern of hydrogen bonding for the  $\text{C}_{18}\text{Gly}_3\text{OEt}$  monolayer. Dotted lines show hydrogen bonds.

tide conformation at an interface. The oligoglycine moiety in the monolayer forms packed hydrogen bonding structures similar to that of polyglycine II as evidenced by the common IR features. The maintenance of a specific conformation for short peptides (Gly<sub>3</sub> to Gly<sub>5</sub>) is interesting, since it is not usually probable in bulk solution. This must be caused by conformational fixation through intermolecular hydrogen bonding. On the other hand, the conformational fixation may reflect the unique nature of the interface. If this contribution is significant, short peptide chains on the biological molecular surface may assume specific (functionally important) conformations that are not probable at non-interfacial sites.

We thank Professor M. Ohno and Professor Y. Shimohigashi of Kyushu University for their kind help and expert discussion on peptide synthesis.

## References

- 1) K. Fujiita, S. Kimura, Y. Imanishi, E. Rump, and H. Ringsdorf, *Langmuir*, **10**, 2731 (1994).
- 2) N. Van Mau, B. Bonet, A. Benayad, and F. Heitz, *Eur. Biophys. J.*, **22**, 447 (1994).
- 3) A. M. Batenburg and R. Brasseur, *J. Biol. Chem.*, **263**, 4202 (1988).
- 4) C. R. Flach and J. W. Brauner, *Biophys. J.*, **67**, 402 (1994).
- 5) B. R. Malcolm, *Biochem. J.*, **110**, 733 (1968).
- 6) K. S. Birdi, in "Lipid and Biopolymer Monolayers at Liquid Interfaces," Plenum Press, New York (1989), Chap. 5.
- 7) A. L. Weisenhorn, D. U. Romer, and G. P. Lorenzi, *Langmuir*, **8**, 3145 (1992).
- 8) N. Higashi, M. Shimoguchi, and M. Niwa, *Langmuir*, **8**, 1509 (1992).
- 9) U. Röthlisberger, M. L. Klein, and M. Sprik, *J. Mater. Chem.*, **4**, 793 (1994).
- 10) J. Umemura, T. Kamata, T. Kawai, and T. Takenaka, *J. Phys. Chem.*, **94**, 62 (1990).
- 11) H. W. Thompson, D. L. Nicholson, and L. N. Short, *Discuss. Faraday Soc.*, **9**, 222 (1950).
- 12) E. R. Blout and S. G. Linsley, *J. Am. Chem. Soc.*, **74**, 1946 (1952).
- 13) L. J. Bellamy, in "The Infrared Spectra of Complex Molecules," 3rd ed, Chapman and Hall, London (1975), Vol. I, pp. 231–258.
- 14) F. H. C. Crick and A. Rich, *Nature (London)*, **176**, 780 (1955).
- 15) G. N. Ramachandran, V. Sasisekharan, and C. Ramakrishnan, *Biochim. Biophys. Acta*, **112**, 168 (1966).
- 16) B. Lotz, *J. Mol. Biol.*, **87**, 169 (1974).
- 17) J. Bandekar and S. Krimm, *Biopolymers*, **27**, 909 (1988).
- 18) E. W. Hughes and W. J. Moore, *J. Am. Chem. Soc.*, **71**, 2618 (1949).
- 19) O. Hirofuji and O. Kunihiro, *J. Phys. Chem.*, **93**, 6638 (1989).
- 20) G. M. Bonora, C. Toniolo, and V. N. R. Pillai, *Gazz. Chim. Ital.*, **110**, 503 (1980).
- 21) W. W. Cleland and M. M. Kreevoy, *Science*, **264**, 1887 (1994).
- 22) W. H. Moore and S. Krimm, *Biopolymers*, **15**, 2439 (1976).
- 23) A. M. Dwivedi and S. Krimm, *Biopolymers*, **21**, 2377 (1982).
- 24) S. Krimm and K. Kuroiwa, *Biopolymers*, **6**, 401 (1968).
- 25) A. M. Dwivedi and S. Krimm, *Macromolecules*, **15**, 177 (1982).
- 26) A. E. Martell and M. K. Kim, *J. Coord. Chem.*, **4**, 9 (1974).
- 27) Y. Abe and S. Krimm, *Biopolymers*, **11**, 1817 (1972).
- 28) G. D. Fasman, in "Poly- $\alpha$ -Amino Acids," Marcel Dekker, New York (1967), p. 599.